Planetary Nebulae: A Universal Toolbox in the Era of Precision Astrophysics
Proceedings IAU Symposium No. 384, 2025
O. De Marco, A. Zijlstra & R. Szczerba, eds.
doi:10.1017/S1743921323005586

Using adaptive-optics assisted MUSE observations to measure galaxy distances with the Planetary Nebula luminosity function

Saskia Schlagenhauf[1,2] and Marc Sarzi[1]

[1]Armagh Observatory and Planetarium, UK
email: saskia.schlagenhauf@armagh.ac.uk

[2]Queen's University Belfast, UK

Abstract. Thanks to its characteristic bright cut-off, the planetary nebulae luminosity function (PNLF) has now become a well-established extragalactic distance indicator that is in principle applicable to all types of galaxies. Most recently, several studies have demonstrated how the use of integral-field spectroscopy can lead to even more precise PNLF measurements, in particular as it allows to probe the central regions of galaxies and obtain well-sampled PNLF distributions. In this respect, adaptive optics (AO) is expected to further increase the scope and reach of PNLF measurements, as it should allow for the detection of even more and more distant PNe. This proceeding presents first results of the investigation of the MUSE-AO performance in relation to the detection of PNe in external galaxies, based on all galaxies with wide-field mode AO observations in the ESO archive.

Keywords. instrumentation: adaptive optics, planetary nebulae, galaxies: distances, galaxies: luminosity function

1. Introduction

Planetary nebulae have extraordinary bright [OIII] emission, especially the λ5007 line, which makes them detectable even in external galaxies, where they appear as unresolved point sources. So far, PNe have been detected as far as 100 Mpc in the Coma cluster, which makes them the second most distant single-star phenomena whose spectrum can be analysed with 8-m class telescopes, after cosmological supernovae (Arnaboldi and Gerhard 2022). This has allowed to collect samples of PNe in well-studied systems to which we know the distance, e.g. Large and Small Magellanic Cloud, Andromeda and the Leo galaxy group. Ciardullo et al. (1989) analysed PNe in our local group and found that the planetary nebulae luminosity function (PNLF) could be described as:

$$N(M) \propto e^{0.307M} \cdot \left(1 - e^{3(M^* - M)}\right), \tag{1.1}$$

with the number of PNe N, the absolute magnitude of the PN M, and the absolute magnitude cutoff M^*. What is most remarkable about this relation is its sharp brightness cutoff, at $M^* = -4.48$. This makes it possible to determine the distance to a galaxy, in which we can detect enough PNe to determine the apparent magnitude of this cutoff. To do so, it is necessary to convert the λ5007 line flux F_{5007} into and equivalent V-magnitude m_{5007} using

$$m_{5007} = -2.5 \log (F_{5007}) - 13.74 \tag{1.2}$$

from Jacoby (1989).

Table 1. Target galaxies observed with MUSE. For each galaxy, right ascension (RA), declination (Dec), and the Hubble distance D is given. The Hubble distances are taken from the NASA/IPAC Extragalactic Database (NED)[1], where the Hubble distance is determined by assuming a Hubble constant of $67.8\,\mathrm{km\,s^{-1}\,Mpc^{-1}}$.

Target	RA	Dec	D [Mpc]
NGC 0244	00°45′46″	−15°35′47″	9.26 ± 0.72
NGC 1336	03°26′32″	−35°43′21″	19.34 ± 1.36
NGC 6958	20°48′43″	−37°59′50″	36.96 ± 2.60
NGC 1326	03°23′56″	−36°27′52″	18.47 ± 1.30
NGC 1553	04°16′10″	−55°46′49″	15.74 ± 1.11
NGC 1440	03°45′03″	−18°15′60″	21.85 ± 1.59
NGC 3489	11°00′18″	+13°54′03″	15.09 ± 1.12
NGC 3412	10°50′53″	+13°24′42″	17.51 ± 1.28
NGC 3593	11°14′37″	+12°49′05″	14.32 ± 1.07
NGC 1079	02°43′44″	−29°00′12″	18.87 ± 1.34
NGC 1201	03°04′08″	−26°04′11″	22.58 ± 1.60
NGC 1320	03°24′49″	−03°02′32″	38.64 ± 2.71
NGC 3626	11°20′04″	+18°21′24″	26.98 ± 1.92
NGC 4457	12°28′59″	+03°34′15″	18.09 ± 1.32
NGC 4379	12°25′15″	+15°36′25″	20.63 ± 1.48
NGC 4421	12°27′03″	+15°27′39″	27.66 ± 1.96
NGC 4528	12°34′06″	+11°19′14″	25.18 ± 1.80
NGC 5121	13°24′36″	−37°40′60″	25.73 ± 1.83

[1] https://ned.ipac.caltech.edu

The greatest advantage of using the PNLF as a distance indicator is, that it can be applied to all Hubble types of galaxies, since PNe appear in all stellar populations. In comparison, the other two main extra-galactic measurement techniques, surface brightness fluctuations and Cepheid variables, can only be applied to early and late type galaxies, respectively. This makes the PNLF a relatively standard method to derive distances, allowing in principle to be an important calibrator of methods further up in the distance ladder, such as the cosmologically all important Supernovae Ia (SNIa) that indeed occur in all sorts of galaxies (see Riess et al. 2022).

In recent years, integral-field spectroscopy has proven particularly useful to deliver abundant samples of PNe in external galaxies and thus ensure robust PNLF distance measurements, in particular as it allows to detect PNe in the central, PNe-rich regions of galaxies (see e.g. Sarzi et al. 2011). With its relatively large field of view ($1' \times 1'$) and broad spectral range ($465\,\mathrm{nm} \times 930\,\mathrm{nm}$)† the MUSE instrument is ideally suited for PNe detection, as it also allows for the identification of PNe impostors such as compact HII regions and supernovae remnants. Furthermore, the MUSE adaptive optics (AO) system promises to deliver even larger PNe sample at a given distance or to detect PNe in galaxies further away by allowing to detect fainter [OIII] point sources.

2. Galaxy Sample

As of June 2023, in total 18 galaxies were available in the ESO archive that were observed with MUSE in Wide-Field Mode (WFM) using AO (Table 1). For each galaxy, right ascension (RA), declination (Dec), and Hubble distance D is given. Hubble distances are taken from the NASA/IPAC Extragalactic Database (NED). In total, the galaxies have Hubble distances between 9 Mpc and 39 Mpc with a median Hubble distance of 20 Mpc. As indicated in the previous section, galaxies in this distance range can act as valuable calibrators for other distance measurements. However, it is important to note, that the present archival sample comes with a some limitations as not all galaxies are ideally suited for applying the PNLF distance method.

† https://www.eso.org/sci/facilities/paranal/instruments/muse/inst.html

https://doi.org/10.1017/S1743921323005586 Published online by Cambridge University Press

3. Data Analysis

To detect and measure the flux of PNe in MUSE data and then obtain a distance based on the PNLF we followed the procedures described in Spriggs et al. (2020, 2021), which were used for MUSE WFM observations without AO.

The procedure starts from obtaining a stellar-continuum subtracted cube, following a spaxel-by-spaxel fit to the MUSE spectra using both the pPXF and GandALF codes (Cappellari and Emsellem 2004; Sarzi et al. 2006) to simultaneously model the stellar and nebular components in the MUSE spectra. Whilst this first analysis of the MUSE cubes already deliver an [OIII] map that generally reveals the presence of several PNe, it is not specifically optimised to identify such sources. Indeed PNe have only modest expansion velocities of a few tens of km/s so that their unresolved line profile will generally be narrower than the one coming from diffuse ionised-gas emission. Once the stellar continuum has been subtracted in each spaxel we therefore proceed to run a dedicated spaxel-by-spaxel fit only the the [OIII]$\lambda\lambda$4959, 5007 doublet imposing a fixed intrinsic line velocity dispersion of 40 km/s (Schönberner et al. 2014) and while also accounting for an instrumental resolution of 75 km/s at 5007 Å (Guérou et al. 2017).

Such a dedicated spaxel-by-spaxel fit gives us a final [OIII] flux emission map and - most important - a map for the ratio between the amplitude (A) of [OIII] emission and the residual-noise level (rN) in each spaxel that we can use to detect PNe candidates, [OIII] point sources using the Python package SEP, which is based on the Sextractor source-finding algorithm by Bertin and Arnouts (1996).

The next step is to validate or reject the identified PNe candidates, whilst also measuring their final flux. To do so a small 9×9 spaxel cube over a restricted wavelength region from 4900 Å to 5100 Å is extracted around each candidate source for a final fit in which all [OIII] lines in the 81 spectra of such a cube are simultaneously fit while imposing the same line profile and a spatially varying overall flux that follows the MUSE point-spread function, as would be expected in the presence of unresolved [OIII] emission from a PN. During this fit, only the overall total flux, velocity and position of such an unresolved [OIII] source is optimised for. Key to this fit, is the prior knowledge of the PSF, which in our case we took to have a Moffat profile (see Moffat 1969), with the shape parameters determined with the pipeline from Fusco et al. (2020).

Such a 1D+2D fit allows to exclude some PNe candidates that are in fact regions with ionised-gas emission or false-positive detections. Spriggs et al. (2020) showed, that sources with a central A/rN > 3 and a sufficient fit quality, which means that the χ^2 value was above the 95% confidence level, can be confirmed as [OIII] point sources and used for further analysis.

As brighter PNe are easier to detect than fainter ones, we have to account for the incompleteness of our PNe sample. Therefore, the PNLF (see Equation 1.1) is modified by the completeness ratio for each magnitude, where the completeness ratio is the fraction of the [OIII] image where a PN with that magnitude could be detected. The completeness corrected PNLF has only one free parameter the apparent magnitude cutoff which yields the distance to the galaxy.

4. Sample Limitations

As we did not chose the sample of galaxies because of their properties, but rather because of what is available in the ESO archive, some galaxies are not ideal for PNe detection. This includes galaxies where a large portion of the MUSE field of view presents diffuse and strong ionized-gas emission (e.g, NGC 1320), leaving only a small and insufficient number of PNe detections for an accurate PNLF distance measurement, similarly to the case of objects that are too far away (e.g., NGC 6958) or that are intrinsically not

https://doi.org/10.1017/S1743921323005586 Published online by Cambridge University Press

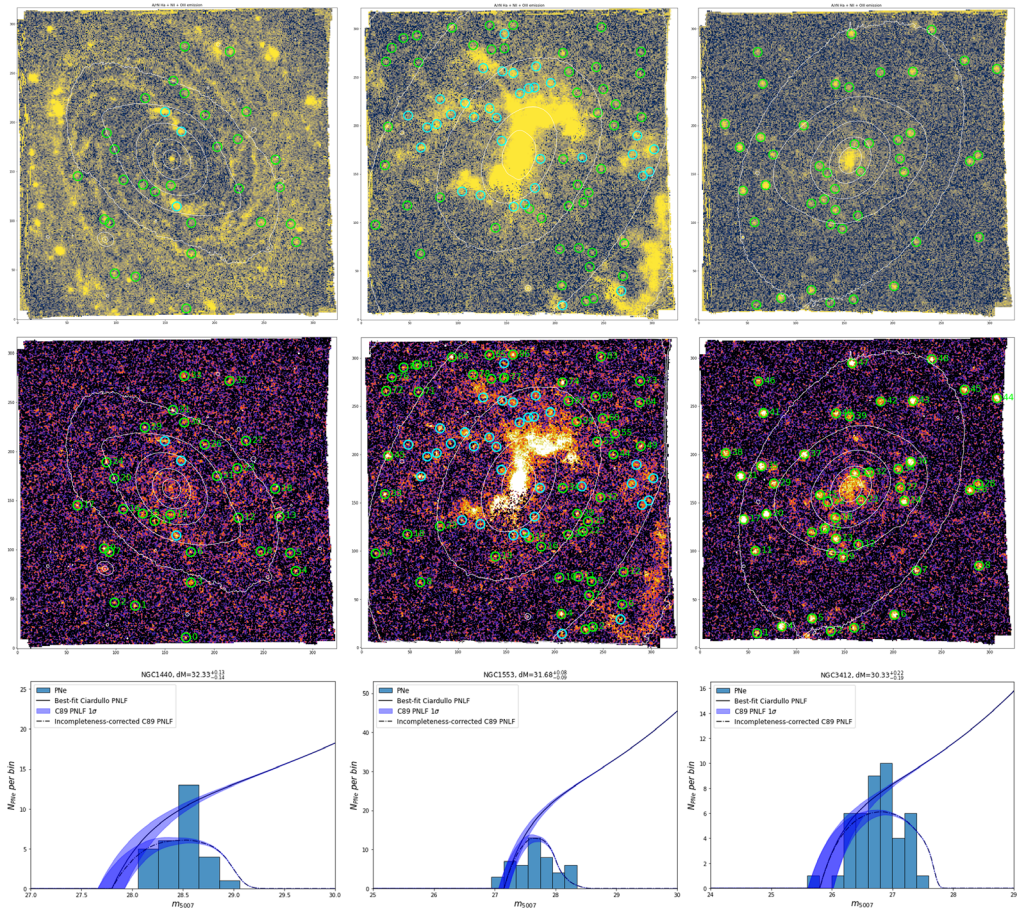

Figure 1. Top: Ar/N map of combined Hα, [NII], and [OIII] emission. The positions of PNe are indicated with green circles, PNe impostors with blue circles. Center: Ar/N map of [OIII] emission. PNe are circled in green, PNe impostors in blue. Bottom: Incompleteness corrected PNLF fit. Galaxies from left to right: NGC 1440, NGC 1553, and NGC 3412.

sufficiently massive to offer abundant PNe populations (e.g., NGC 0244). Work is under way to at least derive robust upper-limits on the distance to such galaxies.

5. First Results

In this Proceeding, we present the distances to the three galaxies NGC 1440, NGC 1553, and NGC 3412. From top to bottom, for each galaxy Figure 1 shows the Ar/N map of the combined Hα, [NII], and [OIII] emission, alerting to the presence of diffuse ionised-gas emission, the Ar/N map of [OIII] emission showing [OIII] point sources and our final PNLF fits. PNe and PNe impostors (HII regions, SNR or PNe too deeply embedded in diffuse gas) are shown by the green and blue circles, respectively. The PNLF show fit with the Ciardullo prescription with and without incompleteness correction. The results of our analysis are summarised in Table 2. For NGC 1440 we found a distance of nearly 30 Mpc at a 6 % accuracy, which effectively pinpoint the location of this object whose previous distance estimates ranged widely between 18 Mpc to 83 Mpc. Furthermore, the accuracy of our distance measurement is comparable to the typical accuracy of the non-AO observations of Spriggs et al. (2021) for Fornax cluster galaxies at 20 Mpc, thus demonstrating the usefulness of AO data in this game. For NGC 3412, the PNLF agrees

https://doi.org/10.1017/S1743921323005586 Published online by Cambridge University Press

Table 2. Results determined from the PNLF fit.

Target	#PNe	dM [mag]	D [Mpc]	D_{ref} [Mpc]	Type	Reference
NGC 1440	29	$32.332^{+0.126}_{-0.138}$	29.26 ± 1.80	18 - 83	TF, FJ	[1,2]
NGC 1553	47	$31.683^{+0.076}_{-0.086}$	21.71 ± 0.85	18.3	SBF	[3]
NGC 3412	44	$30.332^{+0.225}_{-0.193}$	11.65 ± 1.28	11.3	SBF	[3]

TF: Tully-Fisher, FJ: Faber-Jackson, SBF: Surface brightness fluctuations
[1]de Vaucouleurs and Olson (1984), [2]Tully and Fisher (1988), [3]Tully et al. (2013)

with the measurements from surface brightness fluctuations, whereas for NGC 1553 the PNLF gives a slightly larger distance than surface brightness fluctuations.

6. Outlook

Other studies have been carried out with MUSE data using the Differential Emission Line Filter (DELF) technique (Roth et al. 2021) that are generally consistent with our approach (Jacoby et al. 2023). DELF provides excellent results by using less computational resources but our approach may prove more versatile when it will come to disentangling PNe from diffuse ionised-gas emission (see Pastorello et al. 2013) or blended PNe in the crowded central regions of galaxies, thanks to the possibility to account for the separate kinematics of such components. In a coming paper we will complete our analysis of all galaxies available in the ESO archive observed with MUSE in wide field mode using AO to fully assess its usefulness for PNLF distance measurements.

References

Arnaboldi, M. & Gerhard, O. 2022, Kinematics of the diffuse intragroup/intracluster light in groups and clusters of galaxies in the Local Universe (within 100 Mpc distance). Frontiers in Astronomy and Space Sciences, 9, 403.

Bertin, E. & Arnouts, S. 1996, Sextractor: Software for source extraction. Astron. Astrophys. Suppl. Ser., 117(2), 393–404.

Cappellari, M. & Emsellem, E. 2004, Parametric Recovery of Line-of-Sight Velocity Distributions from Absorption-Line Spectra of Galaxies via Penalized Likelihood. PASP, 116(816), 138–147.

Ciardullo, R., Jacoby, G. H., & Ford, H. C. 1989, Planetary Nebulae as Standard Candles. IV. A Test in the Leo I Group. APJ, 344, 715.

de Vaucouleurs, G. & Olson, D. W. 1984, A comparison of distance scales for early-type galaxies. APJS, 56, 91–104.

Fusco, T., Bacon, R., Kamann, S., Conseil, S., Neichel, B., Correia, C., Beltramo-Martin, O., Vernet, J., Kolb, J., & Madec, P. Y. 2020, Reconstruction of the ground-layer adaptive-optics point spread function for MUSE wide field mode observations. AAP, 635, A208.

Guérou, A., Krajnović, D., Epinat, B., Contini, T., Emsellem, E., Bouché, N., Bacon, R., Michel-Dansac, L., Richard, J., Weilbacher, P. M., Schaye, J., Marino, R. A., den Brok, M., & Erroz-Ferrer, S. 2017, The MUSE Hubble Ultra Deep Field Survey. V. Spatially resolved stellar kinematics of galaxies at redshift $0.2 \lesssim z \lesssim 0.8$. AAP, 608, A5.

Jacoby, G. H. 1989, Planetary Nebulae as Standard Candles. I. Evolutionary Models. APJ, 339, 39.

Jacoby, G. H., Ciardullo, R., Roth, M. M., Arnaboldi, M., & Weilbacher, P. M. 2023, Towards Precision Cosmology With Improved PNLF Distances Using VLT-MUSE II. A Test Sample from Archival Data. arXiv e-prints, arXiv:2309.11603.

Moffat, A. F. J. 1969, A Theoretical Investigation of Focal Stellar Images in the Photographic Emulsion and Application to Photographic Photometry. AAP, 3, 455.

Pastorello, N., Sarzi, M., Cappellari, M., Emsellem, E., Mamon, G. A., Bacon, R., Davies, R. L., & de Zeeuw, P. T. 2013, The planetary nebulae population in the nuclear regions of M31: the SAURON view. MNRAS, 430(2), 1219–1229.

https://doi.org/10.1017/S1743921323005586 Published online by Cambridge University Press

Riess, A. G., Yuan, W., Macri, L. M., Scolnic, D., Brout, D., Casertano, S., Jones, D. O., Murakami, Y., Anand, G. S., Breuval, L., Brink, T. G., Filippenko, A. V., Hoffmann, S., Jha, S. W., D'arcy Kenworthy, W., Mackenty, J., Stahl, B. E., & Zheng, W. 2022, A Comprehensive Measurement of the Local Value of the Hubble Constant with 1 km s^{-1} Mpc^{-1} Uncertainty from the Hubble Space Telescope and the SH0ES Team. APJL, 934(1), L7.

Roth, M. M., Jacoby, G. H., Ciardullo, R., Davis, B. D., Chase, O., & Weilbacher, P. M. 2021, Toward Precision Cosmology with Improved PNLF Distances Using VLT-MUSEI. Methodology and Tests. APJ, 916(1), 21.

Sarzi, M., Falcón-Barroso, J., Davies, R. L., Bacon, R., Bureau, M., Cappellari, M., de Zeeuw, P. T., Emsellem, E., Fathi, K., Krajnović, D., Kuntschner, H., McDermid, R. M., & Peletier, R. F. 2006, The SAURON project - V. Integral-field emission-line kinematics of 48 elliptical and lenticular galaxies. MNRAS, 366(4), 1151–1200.

Sarzi, M., Mamon, G. A., Cappellari, M., Emsellem, E., Bacon, R., Davies, R. L., & de Zeeuw, P. T. 2011, The planetary nebulae population in the central regions of M32: the SAURON view. MNRAS, 415(3), 2832–2843.

Schönberner, D., Jacob, R., Lehmann, H., Hildebrandt, G., Steffen, M., Zwanzig, A., Sandin, C., & Corradi, R. L. M. 2014, A hydrodynamical study of multiple-shell planetary nebulae. III. Expansion properties and internal kinematics: Theory versus observation. Astronomische Nachrichten, 335(4), 378–408.

Spriggs, T. W., Sarzi, M., Galán-de Anta, P. M., Napiwotzki, R., Viaene, S., Nedelchev, B., Coccato, L., Corsini, E. M., Fahrion, K., Falcón-Barroso, J., Gadotti, D. A., Iodice, E., Lyubenova, M., Martín-Navarro, I., McDermid, R. M., Morelli, L., Pinna, F., van de Ven, G., de Zeeuw, P. T., & Zhu, L. 2021, The Fornax3D project: Planetary nebulae catalogue and independent distance measurements to Fornax cluster galaxies. AAP, 653, A167.

Spriggs, T. W., Sarzi, M., Napiwotzki, R., Galán-de Anta, P. M., Viaene, S., Nedelchev, B., Coccato, L., Corsini, E. M., de Zeeuw, P. T., Falcón-Barroso, J., Gadotti, D. A., Iodice, E., Lyubenova, M., Martín-Navarro, I., McDermid, R. M., Pinna, F., van de Ven, G., & Zhu, L. 2020, Fornax 3D project: Automated detection of planetary nebulae in the centres of early-type galaxies and first results. AAP, 637, A62.

Tully, R. B., Courtois, H. M., Dolphin, A. E., Fisher, J. R., Héraudeau, P., Jacobs, B. A., Karachentsev, I. D., Makarov, D., Makarova, L., Mitronova, S., Rizzi, L., Shaya, E. J., Sorce, J. G., & Wu, P.-F. 2013, Cosmicflows-2: The Data. AJ, 146(4), 86.

Tully, R. B. & Fisher, J. R. 1988,. Catalog of Nearby Galaxies. Cambridge University Press.